J Electr Eng Technol.2015; 10(4): 1674-1681
http://dx.doi.org/10.5370/JEET.2015.10.4.1674

ISSN(Print) 1975-0102
ISSN(Online) 2093-7423

Improved Method for Calculating Armature-Reaction Field of Surface-Mounted Permanent Magnet Machines Accounting for Opening Slots

Yu Zhou†, Huaishu Li*, Qingyu Wang*, Zhiqiang Xue*, Qing Cao* and Shi Zhou*

Abstract – This paper presented an improved analytical method for calculating armature-reaction field in the surface-mounted permanent magnet machines accounting for opening slots. The analytical model is divided into two types of subdomains. The current of the armature is centralized in the center of the slots. The field solution of each subdomain is obtained by applying the interface and boundary conditions of the model. Two 30-pole/36-slot prototype machines with different slot-opening width are used for validation. The FE (finite element) results confirm the validity of the analytical results with the proposed model. The investigation shows that the wider the slot-opening width is, the smaller the peak value of radial and circumferential components of flux density, and the analytical armature-reaction field produced by centralized current in the slots is similar with the armature-reaction field produced by distributed current in the slots in the FE.

Keywords: Permanent magnet machines, Armature-reaction field, Opening slot, Subdomain model

1. Introduction

Permanent-magnet machines have become more and more popular in the commercial, industrial and military products benefiting from higher power ratio to mass, torque ratio to volume, efficiency and lower vibration and noise over conventional electrically excited synchronous machines and asynchronous machines [1-3]. The magnetic field is one of the most important issues in the permanent-magnet machines. It influences the performance of the motor such as torque ripple [4], armature winding inductances [5, 6], acoustic noise and vibration spectra [7], radial force distribution [8, 9], etc. Its accurate prediction can significantly facilitate and expedite their optimal design in terms of efficiency, compactness, cost and reliability. At the present time, the numerical methods for magnetic field calculation, such as finite-elements method, provide accurate results concerning all kinds of magnetic sizes of permanent magnet machines, taking into account the saturation and without making any simplification of the geometry. But the numerical methods are very time-consuming, not suit to the initial design and optimization of the machines. Usually, the numerical methods are very good for the adjustment and validation of the design. Furthermore, the results which are obtained by numerical methods may be not accurate to calculate cogging torque and unbalanced magnetic force [10, 11] since it is sensitive to the FE meshes. Indeed, the motor performance can be obtained by the analytical methods of field computation based on the sufficient hypotheses [12].

Carter's coefficient has been widely used to consider the slotting effects in conventional electrically excited synchronous machines and asynchronous machines [3, 13]. Its accuracy is not enough sometimes. The current of armature winding is equivalent to the distributed current sheet in the inner surface of the stator by Zhu et al. [14]. Then he proposed the analytical method accounting for stator slot openings by the application of the conformal transformation method and a "2-d" relative permeance function [15]. Zarko [16] introduced the notion of complex relative air-gap permeance, calculated from the conformal transformation of the slot geometry, to take into account the effect of slotting. This solution follows directly from the Schwarz-Christoffel transformation, which is a complex function by nature.

Zhu [5] proposed distributed current area, and divided the field domain into two regions: the region with air-gap and magnet and the region with slotless winding. The accuracy of the 2-D model depended on the assumed radial location of the equivalent current sheet. Wu [17] calculated armature-reaction field of surface-mounted permanent-magnet machines accounting for tooth-tips. The field domain is divided into three types of subdomains. The subdomain model predicted similar flux density in the air gap and magnets, but exhibited much higher accuracy for the flux density in the slots. Its solution is complicated. Rahideh [18] presented analytical armature-reaction field distribution of slotted brushless machines with surface inset permanent magnets. Overlapping and non-overlapping windings with all teeth or alternate teeth were also studied.

In this paper, an improved analytical method accounting for opening slots is derived for calculating the armature-

† Corresponding Author: College of Electrical Engineering, Naval University of Engineering, Wuhan, China. (zhouyu_engineer@hotmail.com)
* College of Electrical Engineering, Naval University of Engineering, Wuhan, China. (249988184@qq.com)
Received: July 3, 2014; Accepted: April 14, 2015

reaction field distribution of machine. In the derivation, the current in the slot is centralized in the center of the slot. The field domain is divided into two types of subdomains: (1) permanent magnet and air-gap; (2) Slots. The analytical field expressions of two subdomains excited by armature windings are obtained by the variable separation method. The coefficients in the expressions are determined by applying the interface and boundary conditions. The investigation shows the developed model has high accuracy to calculate the armature-reaction field of surface-mounted permanent magnet machines. And the wider the slot-opening width is, the smaller the peak value of radial and circumferential components of flux density. The FE results verify the validity of the analytical model.

2. Analytical Field Modeling

In this paper, the analytical modeling is based on the following assumptions:

(1) Linear properties of permanent magnet;
(2) Infinite permeable iron materials;
(3) The relative permeability in the PM is equal to air;
(4) Negligible end effect;
(5) Simplified slot as shown in Fig. 1;
(6) The current in the slot is centralized in the center of the slot.

The two-dimensional subdomain model for calculating armature-reaction field is shown in Fig. 1. The magnet field is divided into two types of subdomains for the convenience of analysis: (1) subdomain of permanent magnet and air-gap (The first subdomain is limited by a circle characterized by a R_s radius); (2) subdomain of slots.

2.1 Armature-reaction field in the first type of subdomains

Since in the 2-D field, the vector potential has only z-axis component which satisfies Laplace equation in the first type of the subdomains:

$$\frac{\partial A_{z1}{}^2}{\partial r^2}+\frac{1}{r}\frac{\partial A_{z1}}{\partial r}+\frac{1}{r^2}\frac{\partial A_{z1}{}^2}{\partial \theta^2}=0 \tag{1}$$

where A_{z1} is vector potential in the air, r and θ are the radius and he angle between OP and the line of $0°$, which is shown in Fig. 1.

The radial and circumferential components of flux density can be obtained from the vector potential distribution by

$$B_\theta=-\frac{\partial A_z}{\partial r} \quad \text{and} \quad B_r=\frac{1}{r}\frac{\partial A_z}{\partial \theta} \tag{2}$$

where B_r and B_θ are radial and circumferential components of flux density respectively.

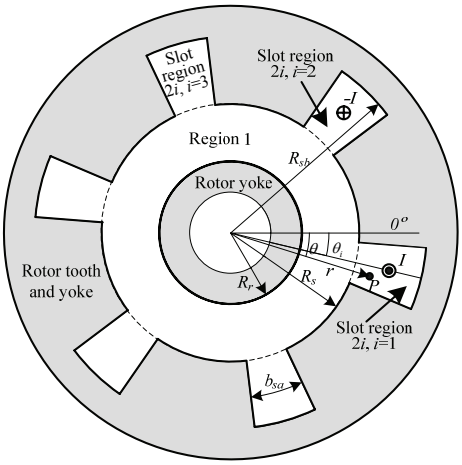

Fig. 1. Symbols and types of subdomains with windings.

In the first type of subdomains, the general solution of (1) can be given by

$$A_{z1}=\sum_{m=1}^{\infty}(A_m^* r^m+B_m^* r^{-m})(C_m^*\cos m\theta+D_m^*\sin m\theta) \tag{3}$$

According to the boundary condition in the first type of subdomain, the circumferential component of flux density is zero in the outer surface of rotor. So

$$B_m^*=A_m^* R_r{}^{2m} \tag{4}$$

where m is the harmonics of the armature-reaction field in the air-gap, and R_r is the radius of the outer surface of rotor.

Substituting (4) into (3), the vector potential in first type of subdomains can be given by

$$\begin{aligned}A_{z1}&=\sum_{m=1}^{\infty}(A_m^* r^m+A_m^* R_r{}^{2m} r^{-m})(C_m^*\cos m\theta+D_m^*\sin m\theta)\\&=\sum_{m=1}^{\infty}F_{2m}(C_m\cos m\theta+D_m\sin m\theta)\end{aligned} \tag{5}$$

where C_m and D_m are coefficients to be determined, and

$$F_{2m}=r^m+R_r{}^{2m} r^{-m} \tag{6}$$

According to (2) and (5), the radial and circumferential components of flux density can be given by

$$B_{r1}=\frac{1}{r}\sum_{m=1}^{\infty}mF_{2m}(-C_m\sin m\theta+D_m\cos m\theta) \tag{7}$$

$$B_{\theta 1}=-\frac{1}{r}\sum_{m=1}^{\infty}F_{1m}(C_m\cos m\theta+D_m\sin m\theta) \tag{8}$$

where B_{r1} and $B_{\theta 1}$ are radial and circumferential components of flux density respectively in the air-gap, and

$$F_{1m} = m(r^m - R_r^{2m} r^{-m}) \tag{9}$$

2.2 Armature-reaction field in the second type of subdomains

The vector potential in the *i*th slot produced by *I* (the current of the winding) can be given by

$$A_{z2i} = -\frac{\mu_0 I}{2\pi}\ln\rho + \sum_{n=1}^{\infty}(A_n^* r^n + B_n^* r^{-n})(C_n^* \cos n\theta + D_n^* \sin n\theta) \tag{10}$$

where μ_0 is permeability of the air, *n* is the harmonics of the armature-reaction field in the slots, and

$$\ln\rho = \begin{cases} -\sum_{n=1}^{\infty}\frac{1}{\mathrm{n}}(\frac{a}{r})^n \cos(n\theta), & r > a \\ -\sum_{n=1}^{\infty}\frac{1}{n}\cos(n\theta), & r = a \\ -\sum_{n=1}^{\infty}\frac{1}{\mathrm{n}}(\frac{r}{a})^{\mathrm{n}} \cos(\mathrm{n}\theta), & r < a \end{cases} \tag{11}$$

where *a* is the distance between windings and the center of the machine.

Boundary conditions in the *i*th slots: ① $B_r = 0$ while $\theta = \theta_i \pm b_{sa}/2$ and $R_s \le r \le R_{sb}$. ② $B_\theta = 0$ while $r = R_{sb}$ and $\theta_i - b_{sa}/2 \le \theta \le \theta_i + b_{sa}/2$ .Where R_s is the radius of the inner surface of stator. R_{sb} is the bottom radius of the slot. b_{sa} is the radian of the each slot.

Then according to boundary conditions, the armature-reaction field produced by the single slot can be solved in the slot. Since the armature-reaction field is symmetrical about the line $\theta = \theta_i$ in the polar coordinates, according to the general solution of (11), the vector potential in the slot can be given as

$$\begin{aligned} A_{z2i} &= -\frac{\mu_0 I}{2\pi}\ln\rho + \sum_{n=1}^{\infty}(A_n^* r^n + B_n^* r^{-n})C_n^* \cos\left[n(\theta-\theta_i)\right] \\ &= -\frac{\mu_0 I}{2\pi}\ln\rho + \sum_{n=1}^{\infty}(A_{ni} r^n + B_{ni} r^{-n})\cos\left[n(\theta-\theta_i)\right] \end{aligned} \tag{12}$$

where A_{ni} and B_{ni} are coefficients to be determined, μ_0 is the permeability of the air, *r* is the radius of point P, θ_i is the angle between center line of the *i*th slot and the line of *0°*.

Then

$$\begin{aligned} A_{z2i} &= \sum_{n=1}^{\infty}[(A_{ni} + \frac{\mu_0 I}{2E_n\pi}a^{-E_n})r^{E_n} \\ &\quad + (A_{ni}R_{sb}^{2E_n} - \frac{\mu_0 I}{2E_n\pi}a^{E_n})r^{-E_n}]\cos[E_n(\theta + \frac{b_{sa}}{2} - \theta_i)] \\ &= \sum_{n=1}^{\infty} F_{1ni}\cos[E_n(\theta + \frac{b_{sa}}{2} - \theta_i)] \end{aligned} \tag{13}$$

for $r < a$, and

$$A_{z2i} = \sum_{n=1}^{\infty}(A_{ni} r^{E_n} + A_{ni} R_{sb}^{2E_n} r^{-E_n})\cos[E_n(\theta + \frac{b_{sa}}{2} - \theta_i)] \tag{14}$$

for $r \ge a$, where

$$F_{1ni} = (A_{ni} + \frac{\mu_0 I}{2E_n\pi}a^{-E_n})r^{E_n} + (A_{ni}R_{sb}^{2E_n} - \frac{\mu_0 I}{2E_n\pi}a^{E_n})r^{-E_n} \tag{15}$$

2.3 Interface conditions between two types of subdomains

2.3.1 The First Interface Condition

The first interface condition is that the circumferential component of the flux density in the inner surface of stator $r = R_s$ is equal.

According to the vector potential distribution in the *i*th slot, the circumferential component of the flux density along the stator bore can be obtained:

$$B_{2i\theta}\big|_{r=R_s} = \sum_{n=1}^{\infty} B_{i\theta n}\cos[E_n(\theta + \frac{b_{sa}}{2} - \theta_i)] \tag{16}$$

where

$$\begin{aligned} B_{i\theta n} &= -\frac{E_n}{R_s}[(A_{ni} + \frac{\mu_0 I}{2E_n\pi}a^{-E_n})R_s^{E_n} \\ &\quad -(A_{ni}R_{sb}^{2E_n} - \frac{\mu_0 I}{2E_n\pi}a^{E_n})R_s^{-E_n}] \\ &= -\frac{E_n}{R_s}(F_{2n}A_{ni} + F_{3n}) \end{aligned} \tag{17}$$

where

$$F_{2n} = R_s^{E_n} - R_{sb}^{2E_n} R_s^{-E_n} \tag{18}$$

$$F_{3n} = \frac{\mu_0 I}{2E_n\pi}\left[\left(\frac{R_s}{a}\right)^{E_n} + \left(\frac{R_s}{a}\right)^{-E_n}\right] \tag{19}$$

The circumferential component of the flux density along the stator bore outside the slot is zero since the stator core material is infinitely permeable. So Fourier series of the circumferential component of the flux density in the inner surface of stator can be given by

$$B_{s\theta 2} = \sum_{m=1}^{\infty}\left[C_{ms}\cos(m\theta) + D_{ms}\sin(m\theta)\right] \tag{20}$$

where

$$C_{ms} = \frac{1}{\pi}\int_0^{2\pi} B_{s\theta 2}\cos(m\theta)d\theta$$
$$= \frac{1}{\pi}\sum_{i=1}^{N_s}\sum_{n=1}^{\infty}\int_{\theta_i-b_{sa}/2}^{\theta_i+b_{sa}/2} B_{i\theta n}\cos\left[E_n(\theta+b_{sa}/2-\theta_i)\right]\cdot\cos(m\theta)d\theta$$
$$= \sum_{i=1}^{N_s}\sum_{n=1}^{\infty} B_{i\theta n}\eta(n,m) \quad (21)$$

$$D_{ms} = \frac{1}{\pi}\int_0^{2\pi} B_{s\theta 2}\sin(m\theta)d\theta$$
$$= \frac{1}{\pi}\sum_{i=1}^{N_s}\sum_{n=1}^{\infty}\int_{\theta_i-b_{sa}/2}^{\theta_i+b_{sa}/2} B_{i\theta n}\cos\left[E_n(\theta+b_{sa}/2-\theta_i)\right]\cdot\sin(m\theta)d\theta$$
$$= \sum_{i=1}^{N_s}\sum_{n=1}^{\infty} B_{i\theta n}\xi(n,m) \quad (22)$$

where

$$\eta(n,m) = -\frac{1}{\pi}\frac{m}{E_n{}^2-m^2}[\cos(n\pi)\sin(m\theta_i+mb_{sa}/2) - \sin(m\theta_i-mb_{sa}/2)] \quad (23)$$

$$\xi(n,m) = \frac{1}{\pi}\frac{m}{E_n{}^2-m^2}[\cos(n\pi)\cos(m\theta_i+mb_{sa}/2) - \cos(m\theta_i-mb_{sa}/2)] \quad (24)$$

According to (8), (20) and the first interface condition, the following equations can be obtained:

$$B_{s\theta 2} = B_{\theta 1}\big|_{r=R_s} \quad (25)$$

Substituting (8), (20) into (25), the following equations can be obtained:

$$\begin{cases} F_{1m}^{r=R_s} C_m = -R_s C_s \\ F_{1m}^{r=R_s} D_m = -R_s D_s \end{cases} \quad (26)$$

Combining (17), (21), (22) and (26), the following equations with matrix format can be obtained:

$$\begin{cases} K_{11}C_1 + K_{13}A_{2i} = Y_1 \\ K_{22}D_1 + K_{23}A_{2i} = Y_2 \end{cases} \quad (27)$$

where

$$K_{11} = diag(F_{11}^{r=R_s}, F_{12}^{r=R_s}, \cdots, F_{1M}^{r=R_s}) \quad (28)$$
$$K_{22} = K_{11} \quad (29)$$
$$K_{13} = -\eta_t^T E_{tn} F_{2tn} \quad (30)$$
$$K_{23} = -\xi_t^T E_{tn} F_{2tn} \quad (31)$$
$$Y_1 = \eta_t^T E_{tn} F_{3tn} \quad (32)$$
$$Y_2 = \xi_t^T E_{tn} F_{3tn} \quad (33)$$
$$\eta_i = (\eta_i(n,m))_{N\times M} \quad (34)$$
$$\eta_t = [\eta_1^T, \eta_2^T, \cdots, \eta_{N_s}^T]^T{}_{(N\cdot N_s)\times M} \quad (35)$$
$$\xi_i = (\xi_i(n,m))_{N\times M} \quad (36)$$
$$\xi_t = [\xi_1^T, \xi_2^T, \cdots, \xi_{N_s}^T]^T{}_{(N\cdot N_s)\times M} \quad (37)$$
$$E_{tn} = diag(E_n, E_n, \cdots, E_n)_{(N\cdot N_s)\times(N\cdot N_s)} \quad (38)$$
$$E_n = diag\left(E_1, E_2 \cdots E_N\right)_{N\times N} \quad (39)$$
$$F_{2tn} = diag(F_{2n}, F_{2n}, \cdots, F_{2n})_{(N\cdot N_s)\times(N\cdot N_s)} \quad (40)$$
$$F_{2n} = diag\left(F_{21}, F_{22}, \cdots, F_{2N}\right)_{N\times N} \quad (41)$$
$$F_{3tn} = [F_{3n}, F_{3n}, \cdots, F_{3n}]^T{}_{(N\cdot N_s)\times 1} \quad (42)$$
$$F_{3n} = [F_{31}, F_{32}, \cdots, F_{3N}]_{1\times N} \quad (43)$$

where $\mathbf{C_1}$, $\mathbf{D_1}$ and $\mathbf{A_{2i}}$ are the column vectors for coefficients C_m, D_m and A_{ni}, e.g. $\mathbf{C_1}=[C_1, C_2, \ldots, C_M]^T$, M is the maximum harmonic order in the air gap and magnet regions, N is the maximum harmonic order in the slot regions and N_s is the number of slots.

2.3.2 The second interface condition

The second interface condition is that the vector potential of the *i*th slot opening is equal in the two types of the subdomains.

According to (5), the vector potential in the inner surface of stator can be given as

$$A_s = A_{z1}\big|_{r=R_s} = \sum_{m=1}^{\infty}\left[A_{mc}\cos(m\theta) + A_{ms}\sin(m\theta)\right] \quad (44)$$

where

$$A_{mc} = F_{2m}^{r=R_s} C_m \quad (45)$$
$$A_{ms} = F_{2m}^{r=R_s} D_m \quad (46)$$

The equation (44) can be expanded into Fourier series along the stator inner surface of the *i*th slot:

$$A_s = \sum_{n=1}^{\infty} A_{ni}\cos[E_n(\theta+b_{sa}/2-\theta_i)] \quad (47)$$

for $\theta_i - b_{sa}/2 \le \theta \le \theta_i + b_{sa}/2$, where

$$A_{ni} = \frac{2}{b_{sa}}\int_{\theta_i-b_{sa}/2}^{\theta_i+b_{sa}/2}\sum_{m=1}^{\infty}[A_{mc}\cos(m\theta) + A_{ms}\sin(m\theta)]\cdot\cos[E_n(\theta+b_{sa}-\theta_i)]d\theta$$
$$= \sum_{m=1}^{\infty}(A_{mc}\sigma_i(n,m) + A_{ms}\tau_i(n,m)) \quad (48)$$

where

$$\sigma_i(n,m)=\frac{2\pi}{b_{sa}}\eta_i(n,m) \tag{49}$$

$$\tau_i(n,m)=\frac{2\pi}{b_{sa}}\xi_i(n,m) \tag{50}$$

According to (14), the vector potential in the inner surface of stator can be obtained:

$$A_{z2i}\big|_{r=R_s}=\sum_{n=1}^{\infty}F_{1ni}^{r=R_s}\cos[E_n(\theta+b_{sa}-\theta_i)] \tag{51}$$

where

$$F_{1ni}^{r=R_s}=F_{4n}A_{ni}+F_{5n} \tag{52}$$

where

$$F_{4n}=R_s{}^{E_n}+R_{sb}{}^{2E_n}R_s{}^{-E_n} \tag{53}$$

$$F_{3n}=\frac{\mu_0 I}{2E_n\pi}\left[\left(\frac{R_s}{a}\right)^{E_n}-\left(\frac{R_s}{a}\right)^{-E_n}\right] \tag{54}$$

According to (47), (53) and the second interface condition, the following equation can be obtained:

$$\sum_{n=1}^{\infty}F_{1ni}^{r=R_s}=\sum_{n=1}^{\infty}\sum_{m=1}^{\infty}(A_{mc}\sigma_i(n,m)+A_{ms}\tau_i(n,m)) \tag{55}$$

Combining (45), (46), (52) and (55), the following equations with matrix format can be obtained:

$$K_{31}C_1+K_{32}D_1+K_{33}A_{2\ i}=Y_3a \tag{56}$$

where

$$K_{31}=\sigma_t diag(F_{21}^{r=R_s},F_{22}^{r=R_s}\cdots F_{2m}^{r=R_s}) \tag{57}$$

$$K_{32}=\tau_t diag(F_{21}^{r=R_s},F_{22}^{r=R_s}\cdots F_{2m}^{r=R_s}) \tag{58}$$

$$K_{33}=-diag(F_{4n},F_{4n},\cdots,F_{4n})_{(N\cdot N_s)\times(N\cdot N_s)} \tag{59}$$

$$Y_3=[G_{5n},G_{5n},\cdots,G_{5n}]^T{}_{(N\cdot N_s)\times 1} \tag{60}$$

$$\sigma_i=(\sigma_i(n,m))_{N\times M} \tag{61}$$

$$\tau_i=(\tau_i(n,m))_{N\times M} \tag{62}$$

$$\sigma_t=[\sigma_1^T,\sigma_2^T\cdots\sigma_{N_s}^T]^T{}_{(N\cdot N_s)\times M} \tag{63}$$

$$\tau_t=[\ \tau_1^T,\ \tau_2^T\cdots\ \tau_{N_s}^T\ ]^T{}_{(N\cdot N_s)\times M} \tag{64}$$

$$F_{4n}=diag\left(F_{41},F_{42},\cdots,F_{4N}\right)_{N\times N} \tag{65}$$

$$F_{5n}=[F_{51},F_{52},\cdots,F_{5N}]_{1\times N} \tag{66}$$

According to (27) and (56), the final equations with matrix format are shown in (67).

$$\begin{bmatrix}K_{11}&0&K_{13}\\0&K_{22}&K_{23}\\K_{31}&K_{32}&K_{33}\end{bmatrix}\begin{bmatrix}C_1\\D_1\\A_{2\ i}\end{bmatrix}=\begin{bmatrix}Y_1\\Y_2\\Y_3\end{bmatrix} \tag{67}$$

Then the coefficients $\mathbf{C_1}$, $\mathbf{D_1}$ and $\mathbf{A_{2i}}$ can be obtained according to (67).

3. Finite-Element Validation

The major parameters of two 30-pole/36-slot prototype machines with different slot-opening width which are used for validation are shown in Table 1. The analytical prediction is compared with the linear FE prediction. The Finite element mesh of the geometry is shown in Fig. 2. The current with 700*A* is distributed in the two slots in FE, while the current with 700*A* is concentrated in the two slots in the analytical method.

Table 1. Parameters of prototype machines (Unit: mm)

Stator outer diameter	520		2P/N_s	30/36
Rotor diameter	370		Stator yoke height	15
Stator inner diameter	400		Active length	460
Slot opening	8	16	Rated speed(rpm)	200

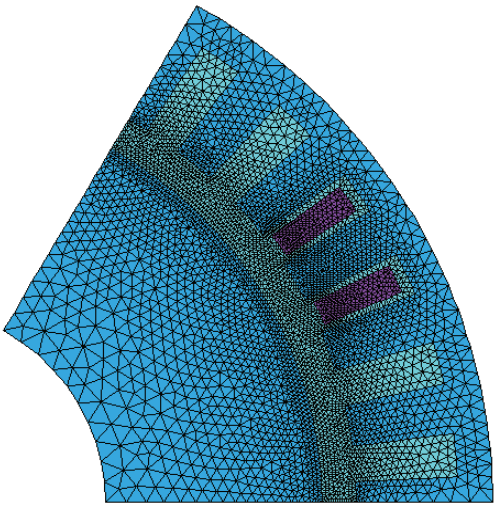

Fig. 2. Finite element mesh of the geometry

Fig. 3 shows the results between analytical and FE predictions of armature-reaction flux density in the air-gap of machine with slot-opening width=8 mm. The peak value of radial component of flux density are 0.083T air-gap r =198mm of motor. And the peak value of circumferential component of flux density are 0.07T in the air-gap r =198mm of motor.

Fig. 4 shows the results between analytical and FE predictions of armature-reaction flux density in the air-gap and slots of machine with slot-opening width =16 mm. The peak value of radial component of flux density are 0.077T

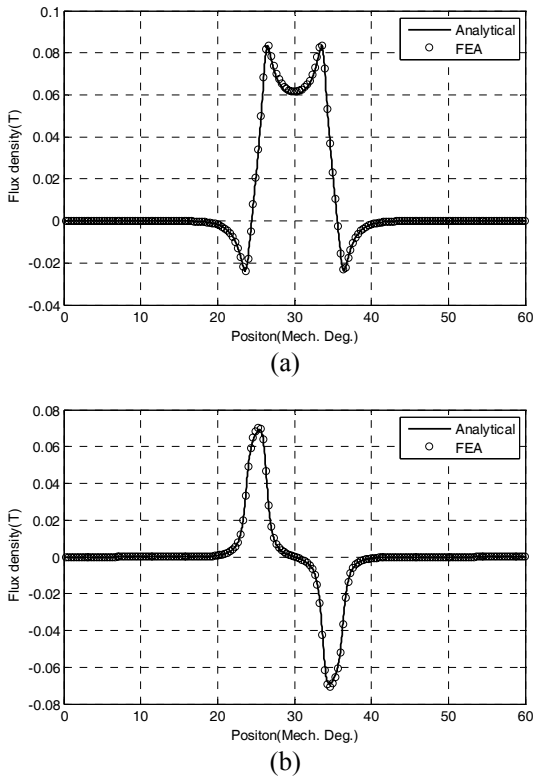

Fig. 3. FE and analytically predicted armature-reaction flux density waveforms in the air-gap r =198mm of motor having slot-opening width =8 mm: (a) Radial component; (b) circumferential component.

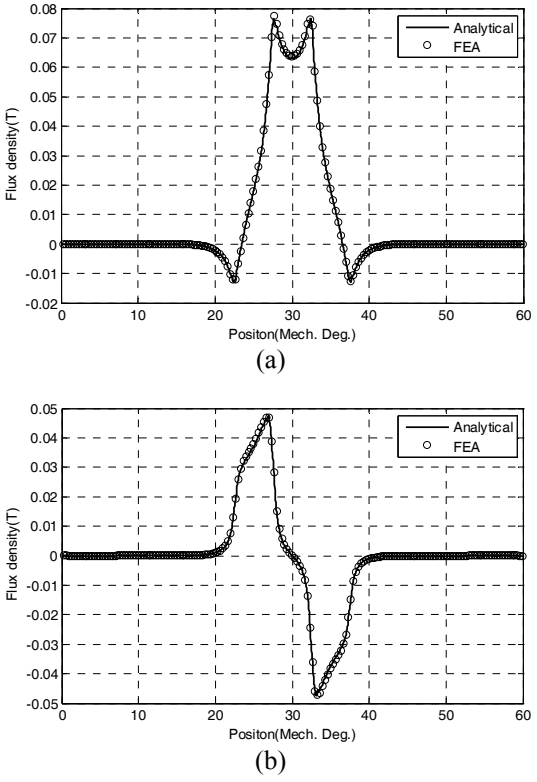

Fig. 4. FE and analytically predicted armature-reaction flux density waveforms in the air-gap r =198mm of motor having slot-opening width=16 mm: (a) Radial component; (b) circumferential component.

in the air-gap r =198mm of motor. And the peak value of circumferential component of flux density are 0.048T in the air-gap r =198mm of motor.

As can be seen from Fig. 3 and Fig. 4, the predicted armature-reaction flux density by subdomain model almost completely matches FE results, and the error is less than 2%. The results show that the wider the slot-opening width is, the smaller the peak value of radial and circumferential components of flux density. At the same time, the analytical armature-reaction field excited by centralized current in the slots is similar with the armature-reaction field excited by distributed current in the slots in the FE.

4. Conclusion

This paper presented an improved method for calculating the armature-reaction field in the surface-mounted permanent magnet machines accounting for slots. The analytical model is divided into two types of subdomains. The current in the slot is centralized in the center of the slot. The field solution of each subdomain is obtained by applying the interface and boundary conditions. The analytical armature-reaction field excited by centralized current in the slots is similar with the armature-reaction field excited by distributed current in the slots with FE method. And the FE results confirm the validity of the analytical results with the proposed model. The investigation shows that the wider the slot-opening width is, the smaller the peak value of radial and circumferential components of flux density.

References

[1] Z. Q. Zhu and D. Howe, "Electrical machines and drives for electric, hybrid, and fuel cell vehicles." *Proc. IEEE*, vol. 95, no. 4, pp. 746-765, Apr. 2007.

[2] Z. Q. Zhu and C. C. Chan, "Electrical machine topologies and tech-nologies for electric, hybrid, and fuel cell vehicles," in *IEEE Vehicle Power and Propulsion Conf.*, 2008, pp. 1-6.

[3] A. M. El-Refaie, "Fractional-slot concentrated-windings synchronous permanent magnet machines: Opportunities and challenges," *IEEE Trans. Ind. Electron.*, vol. 57, no. 1, pp. 107-121, 2010.

[4] I. W. Kim, D. K. Woo and D. K. Lim, "Minimization of a Cogging Torque for an Interior Permanent Magnet Synchronous Machine using a Novel Hybrid Optimization Algorithm," Journal of Electrical Engineering & Technology, vol. 9, no. 3, pp. 859-865, May 2014.

[5] K. Atallah, Z. Q. Zhu, and D. Howe, "Armature reaction field and winding inductances of slotless permanent-magnet brushless machines," IEEE Trans. Magn., vol. 34, no. 5, pp. 3737-3744, Sep. 1998.
[6] Z. Q. Zhu, D. Howe, and T. S. Birch, "Calculation of winding inductances of brushless motors with surface mounted permanents magnets," in *Proc. ICEM*, Paris, France, Sept. 5-8, 1994.
[7] S. B. Yu, and R. Y. Tang, "Electromagnetic and mechanical character-rization of noise and vibration in permanent magnet synchronous machines," *IEEE Trans. Magn.*, vol. 42, no. 4, pp. 1335-1338, Apr. 2006.
[8] J. Wang, Z. P. Xia, S. A. Long, "Radial force density and vibration characteristics of modular permanent magnet brushless ac machine," *IEE Proc. Electric Power Appl.*, vol. 153, no. 6, pp. 793-801, 2006.
[9] Z. Q. Zhu, Z. P. Xia, L. J. Wu, and G. W. Jewell, "Analytical modelling and finite element computation of radial vibration force in fractional-slot permanent magnet brushless machines," *IEEE Trans. Ind. Appl.*, vol. 46, no. 5, pp. 1908-1918, Sep./Oct. 2010.
[10] D. Lin, S. L. Ho, and W. N. Fu, "Analytical Prediction of Cogging Torque in Surface-Mounted Permanent-Magnet Motors," *IEEE Trans. Magn.*, vol. 45, no. 9, pp. 3296-3302, Sep. 2009.
[11] D. H. Wang, X. H. Wang, D. W. Qiao, Y. Pei, and S. Y. Jung, "Reducing Cogging Torque in Surface-Mounted Permanent-Magnet Motors by Nonuni-formly Distributed Teeth Method," *IEEE Trans. Magn.*, vol. 47, no. 9, pp. 2231-2239, Sep. 2011.
[12] Y. Zhou, H. S. Li, W. Wang, Q. Cao and S. Zhou "Improved Method for Calculating Magnetic Field of Surface-Mounted Permanent Magnet Machines Accounting for Slots and Eccentric Magnet Pole," Journal of Electrical Engineering & Technology, vol. 10, no. 3, pp. 1025-1034, May 2015.
[13] N. Boules, "Two-dimensional field analysis of cylindrical machines with permanent magnet excitation," IEEE Trans. Ind. Appl., vol. IA-20, no. 5, pp. 1267-1277, Sep./Oct. 1984.
[14] Z. Q. Zhu and D. Howe, "Instantaneous magnetic field distribution in brushless permanent magnet dc motors. Part II: Armature-reaction field," IEEE Trans. Magn., vol. 29, no. 1, pp. 136-142, Jan. 1993.
[15] Z. Q. Zhu and D. Howe, "Instantaneous magnetic field distribution in brushless permanent magnet dc motors. Part III: Effect of stator slot-ting," IEEE Trans. Magn., vol. 29, no. 1, pp. 143-151, Jan. 1993.
[16] D. Zarko, D. Ban, and T. A. Lipo, "Analytical calculation of magnetic field distribution in the slotted air gap of a surface permanent-magnet motor using complex relative air-gap permeance," IEEE Trans. Magn., vol. 42, no. 7, pp. 1828-1837, Jul. 2006.
[17] L. J. Wu, Z. Q. Zhu, and D. Staton, "An improved subdomain model for predicting magnetic field of surface-mounted permanent-magnet machines accounting for tooth-tips," IEEE Trans. Magn., vol. 47, no. 6, pp. 1693-1704, Jun. 2011.
[18] A. Rahideh and T. Korakianitis, "Analytical Magnetic Field Calculation of Slotted Brushless Permanent-Magnet Machines With Surface Inset Magnets," IEEE Trans. Magn., vol. 48, no. 10, pp. 2633-2649, Oct. 2012.

Yu Zhou was born in China, 1983. He received the B.S. degree and the M.S. degree in electrical engineering from the College of Electrical Engineering, Naval University of Engineering, Wuhan, China in 2005 and 2009 respectively. From 2012, he is working toward the Ph.D. degree in the College of Electrical Engineering, Naval University of Engineering, Wuhan, China. He is one of IEEE Members now. His major research interests include power electronics, and design and control of permanent-magnet machines.

Huaishu Li was born in China, 1965. He received the B.S. degree and the M.S. degree in electrical engineering from the College of Electrical Engineering, Naval University of Engineering, Wuhan, China in 1986 and 1991 respectively, and the Ph.D. degree from Huazhong University of Science & Technology, Wuhan, China in 2001. From 1991, he lectures in the College of Electrical Engineering, Navy University of Engineering, Wuhan, China. His major research interests include power electronics, and design and control of permanent-magnet machines.

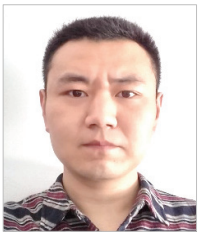

Qingyu Wang was born in China, 1986. He received the B.S. degree in manufacturing and its automation from Tsinghua University, Beijing, China in 2009 and the M. S. degree in navigation from Dalian Naval Academy, Dalian, China in 2011. From 2012, he is working toward the Ph.D. degree in the College of Electrical Engineering, Naval University of Engineering, Wuhan, China. His major research interests include power electronics, and design and control of linear motor.

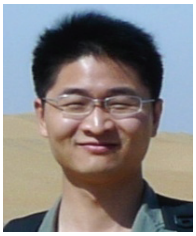

Zhiqiang Xue was born in China, 1979. He received the B.S. degree in electrical engineering and the automatization specialty from the Ordnance Engineering College, Shijiazhuang, China in 2003, and the M.S. degree in electrical engineering from the College of Electrical Engineering, Naval University of Engineering, Wuhan, China in 2009. From 2015, he is working toward the Ph.D. degree in the College of Electrical Engineering, Naval University of Engineering, Wuhan, China. His major research interests include power electronics, and design and control of permanent-magnet machines.

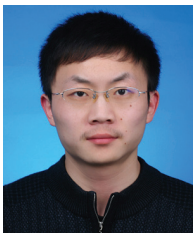

Shi Zhou was born in China, 1988. He received the B.S. degree in physics from Nanjing University, Nanjing, China, in 2011. From 2013, he is working toward the M.S. degree in the College of Electrical Engineering, Naval University of Engineering, Wuhan, China. His research interest is multi-phase permanent-magnetic synchronous generator.

Qing Cao was born in China, 1991. She received the B.S. degree in electric engineering from Hunan Institute of Engineering, Xiangtan, china, in 2013. She is working toward the M.S. in the College of Electrical Engineering, Naval University of Engineering, Wuhan, China. Her research interest is line-start permanent-magnetic synchronous motor.